

Full Length Research Paper

Petrographic and chemical characterization of Fe-Ti oxides and sulfides hosted in mafic intrusions, south Sinai, Egypt: Implication for genesis

Abdel-Aal Mohamed Abdel-Karim

Geology Department, Faculty of Science, Zagazig University, Egypt. E-mail: abdelaalabelkarim@hotmail.com

Accepted 19 May, 2009.

Fe-Ti oxides and Co-Ni-Cu sulfides hosted by younger gabbroic rocks occurring in Imliq, El-Khamila, Wadi Tweiba, Nakhil and Rahaba localities in south Sinai, consist ilmenite, magnetite and titanomagnetite and pyrite, chalcopyrite, pyrrhotite and pentlandite. They often show fine intergrowths, exsolutions or composite grains. Pyrrhotite is replaced by pentlandite or arranged along the amphibole cleavages. The sulfides occur as monomineralic grains included in silicates or attached to the grain boundaries of Fe-Ti oxides. A few sulfide grains are included in or sandwiched by Fe-Ti oxides. The Fe-Ti oxides and sulfides are located in the intercumulus spaces of the host rocks. Exsolution lamellae of magnetite in titanomagnetite or granular exsolution of ilmenite around grains of magnetite were developed by oxidation during cooling of the intrusions. The formation of ilmenite trellis and lamellae in magnetite and titanomagnetite indicates again an oxidation process due to excess of oxygen contained in titanomagnetite; trapped and external oxidizing agents. This indicates the high PH_2O and oxygen fugacity of the parental magma, as suggested by modal increasing of hornblende and biotite and the presence of hypersthene and pigeonite. Addition of crustal sulfur is required to explain the present values of the mineralized gabbros. Sulfide mineralization in present rocks is believed to have resulted from the emplacement of sulfide-saturated tholeiitic and calc-alkaline basaltic magmas that had experienced varying degrees of silicate and sulfide fractionation. These sulfides can be interpreted to have formed by accumulation of immiscible magmatic sulfide droplets. The tholeiitic gabbros dominated in El-Khamila, Wadi Tweiba and Nakhil are characterized by Ni-rich pyrite and chalcopyrite as compared with that of the calc-alkaline gabbros occurring in Imliq and Wadi Nakhil (Ni-poor pyrite and chalcopyrite). A multistage model of ore genesis, involving two stages of crustal contamination, two magma chambers, and multiple pulses of geochemically distinct magma, is entirely consistent with the geochemical data from south Sinai younger gabbros. The Fe-Ti oxides have been formed under temperature of $\sim 800^\circ\text{C}$ for ilmenite and $\sim 600^\circ\text{C}$ for magnetite, while the sulfide assemblage is crystallized below 600°C , with final re-equilibration temperature above 140°C .

Key words: Younger gabbros, Fe-Ti oxides, sulfides, microprobe, P-T conditions, South Sinai, Egypt.

INTRODUCTION

The basement complex of Sinai and Eastern Desert of Egypt splits into four main groups (El-Gaby, 2005): (1) Pre-Pan-African rocks comprising deformed granites, migmatites, gneisses and high-grade metamorphites, (2) Pan-African ophiolite and island arc assemblages thrust onto the old continent, (3) Pan-African Cordillera stage comprising calc-alkaline gabbro-diorite complexes, Dokhan Volcanics, Hammamat sediments, calc-alkaline granite series, together with olivine gabbro and related rocks, and (4) post orogenic to anorogenic alkaline to per-alkaline silicic magmatism including alkali feldspar granites, syenites and alkali rhyolites.

The Egyptian gabbros have been recently classified into three major types (Khalil, 2005): (1) Ophiolitic metagabbros, (2) Arc-related metagabbros and (3) Cordilleran stage gabbros (younger gabbros). The ophiolitic gabbros were termed metagabbro-diorite complex (El-Ramly, 1972) or older metagabbros (Takla et al., 1981). They are regionally metamorphosed and dated 800 - 730 Ma (Kroner et al., 1990). The island arc metagabbros are of limited distribution and difficult to separate them from the ophiolitic metagabbros. The mafic-ultramafic cumulates are intrusive unmetamorphosed rocks (El-Ramly, 1972). They were named fresh, layered younger gabbros

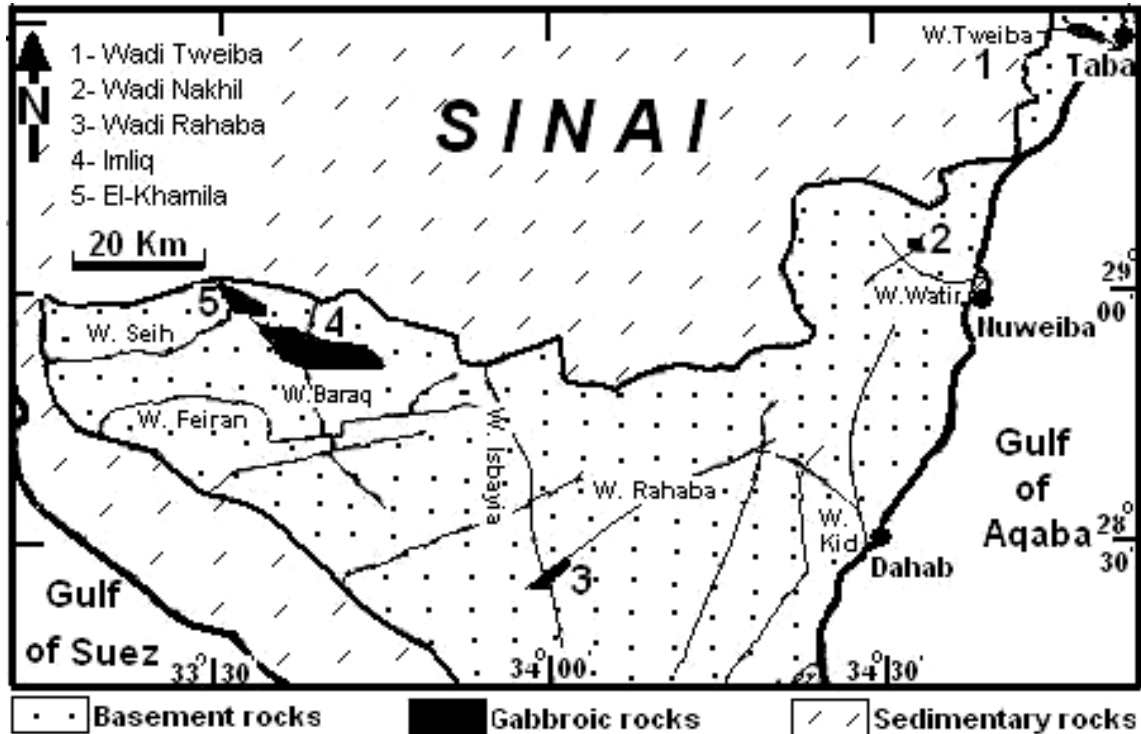


Figure 1. Location map showing the distribution of the studied younger gabbros in south Sinai.

(Takla et al., 1981), and considered to be post-tectonic intrusions (655 - 570 Ma), equivalent to the Andean type calc-alkaline sequence (El-Gaby et al., 1988) or olivine gabbro and related rocks (El-Gaby, 2005).

The mafic intrusions in Sinai Peninsula crop out as numerous small masses. They were metamorphosed into the green-schist facies, and locally in the lower amphibolite. El-Metwally (1997) suggested that the Sinai mafic-ultramafic rocks were intruded in an active continental margin above subduction zone. Takla et al. (2001) considered the most mafic-ultramafics of south Sinai as non ophiolitic assemblage belonging to the Egyptian Younger Gabbros.

The present study focuses on Fe-Ti oxides and sulfide deposits hosted in some mafic intrusions of south Sinai, Egypt in order to shed light on their petrographic and chemical characterization and ore genesis. These mafic intrusions include five minor and isolated younger gabbro masses crop out at Wadis Tweiiba and Nakhil (South-Eastern), Wadi Rahaba (central-Sinai) and Imliq and El-Khamila (southeastern Sinai) (Figure 1). They occur as small irregular elongated masses varying in size from 1.0 km² (Wadi Nakhil) up to 40 km² (Imliq) covering collectively about 61 km².

The iron oxide minerals in the mafic-ultramafic rocks of Egypt have been described by several authors (Takla et al., 1981, 2001; Ramadan and Niazy, 1997; Heikal et al., 1988; Nasr et al., 2000 and others). Most of these studies concentrated on the mode of formation and microscopic investigation.

The sulfide minerals in the mafic-ultramafic rocks of Eastern Desert of Egypt have been studied by Bugrov and Shalaby (1973); Rasmy (1982); Sideek and El-Goresy (1996) and El-Mahallawi et al. (1997). El-Gaby (2005) reported that the Younger, tholeiitic olivine gabbros and related peridotites, proxenites, layered gabbros and meladorites of Egypt are usually associated with Ni-Co-Cu-sulfides and ilmenite deposits. The last authors identified three distinct sulfide assemblages in G. Akarem in the south Eastern Desert: iron-rich monosulfides, pentlandite-iron monosulfides-mackinawite and chalcopyrite-cubanite. No detailed previous studies have been carried out on the sulfides of Sinai. Only geophysical and ore microscopic studies were carried out in the Wadi Sa'al area, south Sinai, to explore the subsurface sulphide mineralization (Mamoun et al., 2004).

General geology and petrography

The Tweiiba gabbros form a small elongated mass, which occupies an area of about 3.2 km². It exhibits a sharp intrusive contact against the adjacent granitoid rocks and schist. The rock is medium grained with massive and equi-dimensional textures. It comprises pyroxene hornblende gabbros in the inner part of the intrusion, and hornblende gabbros in the periphery. Petrographically, the hornblende gabbros are made up of cumulus hornblende and plagioclase, with subordinate amounts of biotite, quartz with accessory Fe oxides, sulfides and apatite. The pyroxene hornblende gabbros are composed

essentially of cumulus hornblende, pyroxene and plagioclase with subordinate amounts of quartz, biotite, and accessory magnetite, ilmenite and apatite.

Wadi Nakhil gabbros form an oval-shape mass (with an area of about 1.0 km²). The mass occurs as large xenoliths or as roof pendants within the neighboring Younger Granites. The rock is fresh, massive and coarse to rarely medium grained and comprises pyroxene-hornblende gabbros and normal gabbros. Petrographically, the hornblende gabbros are essentially composed of cumulus plagioclase (An₅₀₋₅₆) and hornblende with subordinate amounts of intercumulus augite. Quartz, biotite, chlorite apatite and opaques are accessories. The normal gabbros are essentially composed of cumulus plagioclase (An₅₂₋₆₀), augite and intercumulus hornblende with subordinate amounts of biotite. Accessories are quartz, chlorite, apatite and opaques. The pyroxene-hornblende gabbros are essentially composed of cumulus plagioclase (An₅₀₋₅₅) and pyroxene with subordinate amounts of hornblende. Accessories are apatite, magnetite and titanomagnetite.

Wadi Rahaba gabbros occur as a small elongate mass (about 4.2 km²). It comprises uralitized gabbros and hornblendites. The hornblendites form dyke-like bodies cutting across the uralitized gabbros with sharp contacts and extend for about 15 m long and 2.5 widths. Appinitic gabbro variety is also recorded. The Rahaba gabbros display a sharp intrusive contact against and are located within the adjacent tonalite-granodiorite association. The rock is coarse grained with massive and less common schistose textures. Petrographically, the uralitized gabbros are essentially composed of cumulus augite and hypersthene and plagioclase (An₅₄₋₅₉) with subordinate amounts of pigeonite, quartz and accessory apatite, opaques and chlorite. The hornblendites are mainly composed of cumulus hornblende and plagioclase (An₅₂₋₅₇) with minor pyroxene, biotite, quartz and accessories apatite and iron oxides, as well as chlorite as a retrograde mineral.

Imliq gabbros form an irregular elongated mass (~ 50 km²). The mass intrudes calc-alkaline older granitoids and is intruded by alkaline younger granites. Imliq gabbros mainly comprise pyroxene gabbro and leucogabbro. Lenses and dyke-like bodies of clinopyroxenite (10 - 25 m long and 1.0 - 2.5 m width) are observed. It is observed that anorthosite is intruding the gabbro mass. Imliq gabbros are intersected by dyke-swarms of varying composition and styles. Rhythmic layers (a few cm thick) are recorded. The rock is fresh, medium to very coarse-grained. Petrographically, the normal gabbros are basically composed of cumulus plagioclase, pyroxene and hornblende. The accessory phase includes quartz, chlorite, titanomagnetite, apatite and ilmenite. Leucogabbros are essentially composed of cumulus augite, hornblende and intercumulus plagioclase with accessory quartz, chlorite, magnetite, ilmenite and apatite. Ophitic and subophitic intergrowths of plagioclase and hornblende are common. Clinopyroxenites are fundamentally composed of cumulus diopside and its alteration products together with minor

postcumulus plagioclase (An₈₅₋₈₈). The accessories are magnetite, ilmenite, titanite and chalcopyrite.

El-Khamila gabbros occur as an irregular mass (~ 13 km²). The mass intrudes calc-alkaline older granitoids with a sharp intrusive contact. It mainly comprises olivine pyroxene, pyroxene gabbros and less common anorthosite. In places, El-Khamila gabbros exhibit small rhythmic layers (a few cm thick). Igneous lamination is associated with layering. The rock is hard, medium to very coarse-grained, grey to dark green in color. Petrographically, the olivine gabbros are essentially composed of cumulus bytownite (An₆₅₋₇₃), augite and less common olivine. Hypersthene, magnetite, and ilmenite are accessories. Chlorite is the main secondary mineral. The normal gabbros are made up of cumulus labradorite (An₅₂₋₅₈) and augite with minor intercumulus hornblende and pigeonite. Magnetite, apatite, and titanite are the main accessories. The anorthosites consist of cumulus plagioclase (An₇₅₋₈₅), and minor uralitized diopside.

Magnetite and ilmenite are accessories, whereas chlorite and epidote are secondary minerals.

MATERIALS AND METHODS

Thirteen rock samples from the present gabbros were selected and polished for studying the Ti-Fe oxides and sulfides [their textures in the different rock types are given in table (1)].

Electron microprobe analyses of Fe-Ti oxide and sulfide minerals from the five localities were carried out in the Institute of Mineralogy and crystallography, Vienna University. The analytical results of 65 spots of Fe-Ti oxides (35 magnetite, 26 ilmenite and 4 titanomagnetite) and 44 spots of sulfides (14 pyrite, 14 chalcopyrite, 8 pyrrhotite and 8 pentlandite) are given in Tables 2 - 6.

MINERALOGY

I- Ti-Fe oxides

Fe-Ti oxides vary from 5.5 - 7% (El-Khamila gabbros) up to 6.6 - 8.5% (W. Tweiba gabbros) of the whole rocks. The Fe-Ti oxide minerals include magnetite, ilmenite and titanomagnetite (Table 1). Magnetite and ilmenite are the predominant Fe-Ti oxide ore minerals (they are observed in all studied areas).

The Fe-Ti oxides in Tweiba gabbros mainly include titanomagnetite, magnetite and ilmenite forming banded and exsolution textures (Table 3). Titanomagnetite is considered as a primary mineral, forms euhedral crystals enclosed fine lamellae or coarse trellis of magnetite giving rise to banded titanomagnetite-magnetite inter-growth (Figure 2a). The latter intergrowth is composed of number of straight, closely-spaced, parallel bands of magnetite in titanomagnetite (Figure 2a). Similar textures were reported on the younger gabbros of the Eastern Desert (Basta and Takla, 1974; Takla et al., 1981) and of Sinai

Table 1. Distribution of Fe-Ti oxides and sulfides and their intergrowths in the younger gabbros of south Sinai.

Locality	Petrographic nomenclature	Total Fe-Ti oxides	Total sulfides	Ilmenite			Titanomagnetite-magnetite intergrowth				Magnetite			Sulphides		
				Homogeneous ilmenite	With magnetite exsolution	Composite	lamellae (trellis) exsolution	Composite	Fine network	Sandwich	Homogeneous magnetite	Titanomagnetite	Pyrite	Chalcopyrite	Pyrrhotite	Pentlandite
W. Tweiba	Hornblende gabbro	6.6	6.5	-	x	-	xx	-	-	-	xx	x	xxx	xxx	xx	xx
	Pyroxene hornblende gabbro	8.0	5.6	-	x	-	x	-	-	-	x	xx	xxx	xx	xx	xx
W. Nakhil	Hornblende gabbro	5.6	5.5	xx	-	-	xx	xxx	-	-	xxx	x	xx	x	xxx	xx
	Pyroxene gabbro	6.2	3.5	xx	xx	-	xx	xx	-	-	x	x	xx	xx	xx	x
	Olivine pyroxene gabbro	6.6	5.3	x	xx	-	xxx	xxx	-	-	xx	x	xx	xx	xx	xx
W. Rahaba	Hornblende pyroxene gabbro	7.5	6.0	xxx	xx	-	xxx	-	xxx	xxx	x	xx	xx	xx	x	-
	Hornblendite	5.1	4.5	x	xxx	-	xx	-	xxx	xxx	xxx	xx	xx	x	x	-
Imliq	Normal gabbro	6.2	4.0	xx	-	xxx	xxx	-	x	-	xxx	xx	xx	xx	-	-
	Leucogabbro	3.7	3.4	x	-	xx	xxx	-	xxx	-	xx	xx	xx	xx	-	-
	Clinopyroxenite	8.2	3.5	xxx	-	xx	xx	-	xx	-	xx	x	xx	xxx	-	-
El-Khamila	Olivine gabbro	7.0	4.5	xx	-	xx	xx	xxx	xxx	-	xx	x	xx	xx	-	-
	Normal gabbro	5.5	3.7	xxx	-	xxx	x	xx	xx	-	-	-	xxx	xx	-	-
	Anorthosite	5.8	2.5	xx	-	xx	xx	xx	xx	-	x	xx	xx	xx	-	-

xxx = Common, xx = fairly common, x = Rare, - = absent.

(Takla et al., 2001). Magnetite occurs as homogeneous euhedral to subhedral minerals.

The Fe-Ti oxides in Wadi Nakhil gabbros constitute about 5.6 - 6.6 vol. %. The oxides mainly include magnetite, titanomagnetite, ilmenite composite and trellis intergrowths (Table 2). Magnetite occurs as cumulus or intercumulus euhedral to subhedral minerals, with commonly homogeneous phase. Sometimes, it forms irregular grains adjacent to or as exsolution lamellae within titanomagnetite to give composite (juxtaposition) or trellis intergrowth (Figure 2b). The fine network of a coarse trellis titanomagnetite-magnetite intergrowth may indicate that the present gabbros were crystallized at high temperature of early differentiated stage. The contact between titanomagnetite and magnetite is sharp, linear, polygonal or curved. The titanomagnetite is mostly convex towards magnetite. Composite grains of titanomagnetite-magnetite in juxtaposition are very common in the Sinai gabbros in the form of cumulus and inter-cumulus grains. Basta and Takla (1974), Takla et al. (1981), and Takla et al. (2001) described similar inter-growths as indication of fresh (younger) gabbros and either with rare or lacking in the ophiolitic metagabbros.

The oxides in Wadi Rahaba gabbros constitute about 5.1- 7.5 vol. %. They include titanomagnetite, magnetite

and ilmenite which exhibit sandwich, network and lamellae exsolution textures (Table 1). Magnetite-ilmenite occurs as homogeneous euhedral to subhedral minerals. Titanomagnetite usually forms homogeneous euhedral crystals or intergrowths with magnetite. Cumulus grains of Ti-magnetite-magnetite sandwich intergrowth (Figure 2c) and network lamellae exsolution are characteristic of the present gabbros. The network lamellae intergrowth grains enclose fine inclusion of silicate minerals (Figure 2d), which may suggest the early crystallization of the present Fe-Ti oxides. Fine network trellis exsolution of ilmenite in titanomagnetite is also recorded.

The Fe-Ti oxides in Imliq gabbros (3.7 - 8.2 vol. %) are mainly composed of fine network trellis and composite intergrowths of magnetite, titanomagnetite and ilmenite (Table 1). Magnetite occurs as euhedral crystals usually fresh and homogeneous phase. The magnetite-ilmenite contact is commonly straight and sharp. Ilmenite is found as homogeneous subhedral grains adjacent to magnetite which gives composite or juxtaposed grains (Figure 2e). Titanomagnetite occurs as irregular grains adjacent to magnetite and ilmenite or within ilmenite (Figure 2e). It exhibits very fine and short laminae to give ilmenite-magnetite fine network intergrowth. The fine network intergrowth is the result of fine lamellae in magnetite to give

Table 2. Results of microprobe analysis of the magnetite of some younger gabbros from south Sinai, Egypt.

	W. Nakhil								El-Khamila							
	1	2	3	4	5	6	7	8	9	10	11	12	13	14	15	16
SiO ₂	0.11	0.21	0.00	0.04	0.68	0.00	0.00	0.16	2.16	0.00	1.24	3.08	0.45	0.26	0.43	0.71
TiO ₂	0.28	0.39	0.28	0.28	1.07	0.27	0.28	0.34	0.69	0.30	0.80	0.58	0.30	1.27	1.59	1.23
Al ₂ O ₃	0.15	0.19	0.00	0.23	0.23	0.62	0.45	0.17	0.00	0.00	0.00	0.00	0.60	2.17	2.10	0.90
Cr ₂ O ₃	0.42	0.33	0.29	0.56	0.29	0.44	0.31	0.38	0.31	0.34	0.32	0.29	0.32	0.32	0.15	0.26
V ₂ O ₃	0.71	0.64	0.86	0.68	0.77	0.73	0.70	0.67	0.34	1.20	0.36	0.32	0.86	0.80	0.20	0.47
FeO ^t	91.05	90.11	90.78	89.99	89.41	89.63	90.39	90.58	87.56	90.59	88.01	87.11	89.79	87.51	87.88	88.56
NiO	0.38	0.39	0.39	0.38	0.38	0.38	0.38	0.39	0.36	0.37	0.34	0.37	0.37	0.38	0.00	0.24
MnO	0.13	0.32	0.31	0.31	0.31	0.31	0.30	0.23	0.31	0.32	0.32	0.30	0.32	0.32	0.17	0.27
MgO	0.00	0.24	0.25	0.24	0.24	0.24	0.24	0.12	1.88	0.00	1.62	2.15	0.25	0.25	0.14	0.67
Σ	93.23	92.83	93.17	92.70	93.38	92.62	93.04	93.03	93.61	93.11	93.01	94.20	93.27	93.29	93.64	93.31
Fe ₂ O ₃	66.78	66.26	67.32	66.48	63.93	66.13	66.81	66.52	62.87	66.68	64.32	61.41	65.43	62.00	60.00	63.25
FeO	30.96	30.49	30.21	30.17	31.89	30.13	30.28	30.72	30.99	30.59	30.13	31.85	30.91	31.73	33.89	31.65
Σ	99.92	99.47	99.91	99.37	99.78	99.24	99.74	99.70	99.91	99.80	99.46	100.36	99.82	99.51	98.66	99.64

Continue.

	W. Rahaba							Imliq							W. Tweiba				
	17	18	19	20	21	22	23	24	25	26	27	28	29	30	31	32	33	34	35
SiO ₂	0.32	0.32	0.19	0.53	0.21	0.39	0.27	0.24	0.40	0.46	0.25	0.39	1.38	0.71	0.70	0.96	0.46	0.41	0.64
TiO ₂	0.27	0.43	0.38	0.79	0.58	0.28	0.46	0.78	0.51	0.91	0.35	0.61	0.64	0.46	0.77	0.96	1.39	0.55	0.55
Al ₂ O ₃	0.04	0.30	0.09	0.77	0.39	0.32	0.28	0.68	0.46	0.64	0.15	0.50	0.18	0.20	0.22	0.94	1.05	0.44	0.29
Cr ₂ O ₃	0.42	0.41	0.41	0.36	0.57	0.37	0.49	0.53	0.41	0.42	0.40	0.31	0.32	0.44	0.36	0.35	0.27	0.36	0.43
V ₂ O ₃	0.50	0.73	0.45	0.62	0.58	0.68	0.60	0.71	0.63	0.53	0.59	0.84	0.59	0.63	0.70	0.56	0.42	0.65	0.63
FeO ^t	90.94	90.74	90.74	88.86	89.65	90.37	90.24	88.55	89.82	89.10	90.75	89.65	88.96	89.48	89.44	88.06	89.06	89.81	89.78
NiO	0.14	0.00	0.27	0.37	0.32	0.25	0.20	0.38	0.27	0.28	0.20	0.33	0.34	0.36	0.37	0.34	0.15	0.28	0.22
MnO	0.41	0.28	0.41	0.26	0.30	0.37	0.29	0.29	0.31	0.29	0.30	0.31	0.32	0.32	0.31	0.31	0.25	0.33	0.26
MgO	0.16	0.16	0.31	0.62	0.27	0.20	0.22	0.24	0.35	0.47	0.19	0.31	0.86	0.55	0.39	0.87	0.33	0.36	0.43
Σ	93.20	93.25	93.26	93.18	92.88	93.23	93.05	92.51	93.15	93.09	93.18	93.23	93.60	93.15	93.26	93.33	93.38	93.20	93.24
Fe ₂ O ₃	66.72	65.87	66.94	64.37	65.47	66.08	65.89	64.01	65.44	64.36	66.51	65.12	63.81	65.14	64.54	63.07	63.26	65.40	65.05
FeO	30.90	31.47	30.51	30.94	30.73	30.91	30.96	30.96	30.94	31.19	30.90	31.05	31.55	30.86	31.37	31.30	32.15	30.96	31.25
Σ	99.89	99.97	99.97	99.63	99.44	99.85	99.66	98.92	99.71	99.54	99.85	99.75	100.00	99.68	99.73	99.65	99.72	99.76	99.76

trellis. El-Khamila gabbros include titanomagnetite, magnetite and ilmenite (5.5 - 7.0 vol. %) as

fine network trellis, composite and myrmekitic intergrowths (Table 1). Titanomagnetite forms irre-

gular grains mostly present as myrmekitic intergrowths with the silicates or as subhedral grains

Table 3. Results of microprobe analysis of the ilmenite and titanomagnetite of some gabbros from south Sinai, Egypt.

	Ti-magnetite				Ilmenite									
	W. Nakhil		Tweiba		W. Nakhil				El-Khamila					
	1	2	3	4	1	2	3	4	5	6	7	8	9	10
SiO ₂	0.23	0.34	0.00	0.43	0.00	0.00	2.55	0.49	0.34	0.36	0.24	0.26	0.30	0.25
TiO ₂	27.16	72.46	61.67	59.90	46.47	50.49	47.74	49.21	50.16	47.71	46.87	47.27	47.29	47.07
Al ₂ O ₃	0.00	0.00	0.00	0.00	0.74	0.00	0.00	0.00	0.00	0.00	0.00	0.00	0.00	0.00
Cr ₂ O ₃	0.28	0.28	0.28	0.26	0.29	0.28	0.28	0.28	0.28	0.29	0.29	0.31	0.29	0.30
V ₂ O ₃	0.50	0.64	0.80	0.59	0.55	0.55	0.55	0.55	0.55	0.64	0.61	0.61	0.62	0.61
FeO ^t	64.90	25.64	36.58	37.78	49.59	45.97	45.79	46.65	46.75	49.67	50.79	49.93	50.23	50.36
CaO	0.21	0.21	0.00	0.00	0.00	0.00	0.00	0.00	0.00	0.00	0.00	0.00	0.00	0.00
MnO	1.20	0.27	0.27	0.40	0.83	2.13	1.92	2.12	1.99	1.21	1.67	1.48	1.44	1.58
MgO	0.27	0.00	0.00	0.25	0.00	0.00	0.00	0.00	0.00	0.00	0.00	0.00	0.00	0.00
Σ	94.75	99.84	99.60	99.62	98.48	99.42	98.83	99.30	100.07	99.88	100.45	99.86	100.18	100.16
Fe ₂ O ₃	47.44	0.00	0.00	0.00	11.62	3.86	2.80	5.23	4.45	9.36	12.08	10.50	10.72	11.29
FeO	22.21	25.64	36.58	37.78	39.14	42.49	43.27	41.94	42.75	41.25	39.92	40.48	40.58	40.20
Σ	99.50	99.84	99.60	99.62	99.64	99.81	99.11	99.82	100.52	100.83	101.67	100.91	101.25	101.29
Σ	100.00	100.00	100.00	100.00	100.00	100.00	100.00	100.00	100.00	100.00	100.00	100.00	100	100

Table 3. Continues

	Ilmenite															
	W. Rahaba				Imliq						W. Tweiba					
	11	12	13	14	15	16	17	18	19	20	21	22	23	24	25	26
SiO ₂	0.84	0.44	0.34	0.24	0.24	0.25	0.19	0.19	1.27	1.52	0.42	0.24	0.24	0.29	0.24	0.24
TiO ₂	52.60	54.56	49.79	50.28	50.03	49.61	50.05	50.21	49.12	48.47	49.68	50.12	50.38	50.39	49.86	49.64
Al ₂ O ₃	0.00	0.00	0.00	0.00	0.00	0.11	0.00	0.00	0.00	0.00	0.00	0.00	0.00	0.00	0.00	0.00
Cr ₂ O ₃	0.32	0.26	0.26	0.28	0.28	0.28	0.28	0.28	0.28	0.28	0.28	0.28	0.28	0.28	0.28	0.28
V ₂ O ₃	0.67	0.56	0.55	0.57	0.57	0.55	0.55	0.55	0.55	0.55	0.55	0.57	0.57	0.57	0.57	0.57
FeO ^t	41.16	42.49	46.93	46.49	46.36	44.77	45.57	45.93	45.88	46.22	46.70	46.53	46.66	46.04	46.40	46.39
CaO	0.00	0.00	0.00	0.00	0.00	0.00	0.00	0.00	0.00	0.00	0.00	0.00	0.00	0.00	0.00	0.00
MnO	3.58	1.31	2.21	2.29	2.28	3.98	3.24	2.56	2.03	2.02	2.05	2.18	2.20	2.40	2.17	2.21
MgO	0.12	0.12	0.00	0.00	0.00	0.00	0.00	0.00	0.00	0.00	0.00	0.00	0.00	0.00	0.00	0.00
ZnO	0.00	0.00	0.00	0.00	0.00	0.00	0.00	0.00	0.00	0.00	0.00	0.00	0.00	0.00	0.00	0.00
Σ	99.29	99.74	100.09	100.15	99.75	99.55	99.88	99.72	99.12	99.06	99.69	99.92	100.32	99.96	99.52	99.33
Fe ₂ O ₃	0.00	0.00	5.25	4.54	4.64	5.34	4.85	4.33	3.33	4.02	4.84	4.63	4.53	3.97	4.73	4.98
FeO	41.16	42.49	42.21	42.41	42.19	39.96	41.20	42.04	42.88	42.60	42.34	42.37	42.59	42.46	42.15	41.91
Σ	99.29	99.74	100.62	100.60	100.21	100.08	100.37	100.16	99.46	99.47	100.17	100.38	100.77	100.36	99.99	99.82

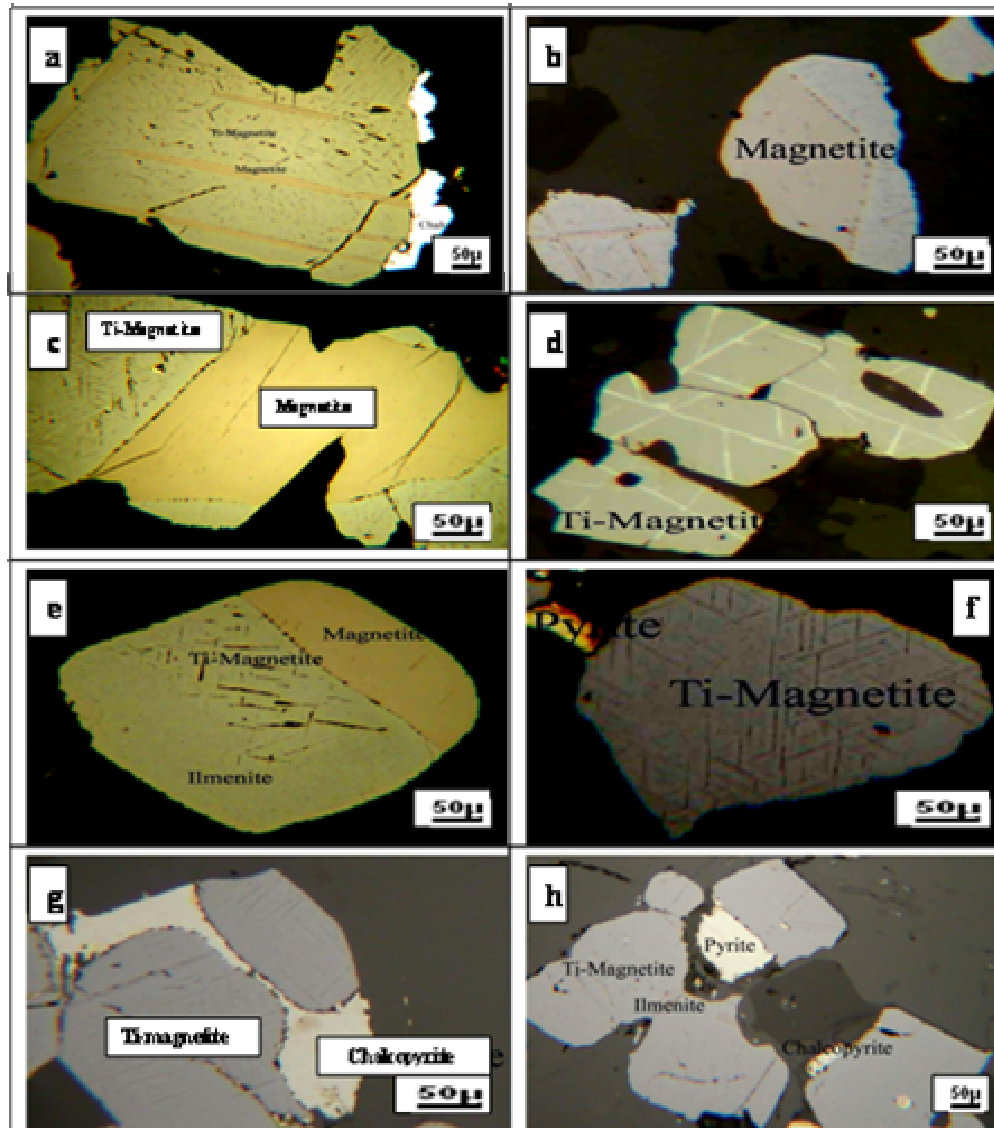


Figure 2. Photomicrographs showing the features of Fe-oxide minerals. **a)** Coarse trellis exsolution (banded) titanomagnetite-magnetite intergrowth, Tweiba, **b)** Trellis lamellae and composite grains of titanomagnetite-magnetite intergrowth, W. Nakhil, **c)** Titanomagnetite-magnetite sandwich intergrowth, Rahaba, **d)** Cumulus grains of titanomagnetite-ilmenite network lamellae exsolution encloses silicate minerals, W. Rahaba, **e)** Euhedral grain of fine network titanomagnetite trellis in between composite ilmenite-magnetite, Imliq, **f)** Ilmenite-titanomagnetite fine trellis exsolution intergrowths, El-Khamila, **g)** Titanomagnetite-chalcopyrite sandwich intergrowth, El-Khamila, **h)** Composite grains of Ti-magnetite-ilmenite and pyrite or chalcopyrite-ilmenite intergrowths, El-Khamila.

adjacent to magnetite to give composite intergrowth.

Fine network lamellae of ilmenite and magnetite display titanomagnetite fine trellis exsolution intergrowths (Figure 2f), which are common in Sinai gabbros. Magnetite occurs as subhedral crystals or irregular grains. Composite grains of homogeneous magnetite and titanomagnetite in juxtaposition are common. Ilmenite occurs as euhedral to anhedral grains mostly forms homogeneous phase. Titanomagnetite-chalcopyrite usually occurs as sandwich intergrowth (Figure 2g). Composite grains of Ti-magnetite-ilmenite and pyrite or chalcopyrite-ilmenite intergrowth

are also recorded (Figure 2h).

II- Sulfides

Sulfides vary from 2.5 - 4.4 vol. % (El-Khamila gabbros) up to 5.6 - 6.5 vol. % (Wadi Tweiba gabbros) of the whole rocks. The sulfides minerals include pyrite, chalcopyrite, pyrrhotite and pentlandite (Table 4). Pyrite and chalcopyrite are the predominant sulphide minerals, founded in all studied areas. Pyrite is the most common secondary sulfide phase. Pyrrhotite and pentlandite are less abundant

Table 4. Results of microprobe analysis of the pyrite of some gabbros from south Sinai, Egypt.

Element %	W. Nakhil			El-Khamila		W. Rahaba			Imliq		W. Tweiba			
	1	2	3	4	5	6	7	8	9	10	11	12	13	14
As	0.05	0.07	0.04	0.12	0.18	0.14	0.13	0.17	0.10	0.05	0.08	0.19	0.18	0.18
Fe	46.97	45.19	46.92	46.69	44.59	46.67	45.85	44.89	46.07	46.36	46.27	46.78	45.98	45.70
Cu	0.04	0.03	0.05	0.04	0.04	0.03	0.05	0.05	0.04	0.04	0.04	0.06	0.04	0.04
Co	0.14	0.13	0.12	0.25	0.22	0.27	0.24	0.24	0.15	0.12	0.16	0.24	0.25	0.24
Ni	0.34	0.29	0.38	0.02	0.02	0.07	0.05	0.04	0.24	0.34	0.23	0.06	0.04	0.05
S	52.05	54.05	52.67	52.34	54.25	52.52	53.21	54.25	53.09	52.92	53.02	52.37	53.04	53.33
Total	99.59	99.76	100.18	99.45	99.30	99.70	99.53	99.64	99.68	99.83	99.79	99.70	99.52	99.54

primary minerals are restricted to Tweiba, Nakhil and Rahaba areas.

The sulfides minerals in Tweiba gabbros occur as pyrite, chalcopyrite and minor pyrrhotite and pentlandite (Table 5). They form small subhedral to anhedral grains disseminated in the mafic minerals. Chalcopyrite encloses minute grains of goethite, usually adjacent to titanomagnetite (Figure 3a). Pyrrhotite forms creamy pinkish brown fine disseminations in the silicates (Figure 3a); flame patches (Figure 3b) or as large anhedral grains commonly enclose pentlandite associated by minute magnetite octahedral grains (Figure 3c). Pentlandite is light cream yellow and usually is present in one or two discrete patches with sharp and irregular margins.

The sulfides in Wadi Nakhil gabbros constitute about 3.5 - 5.5 vol. %. They consist mainly of pyrrhotite and pentlandite and minor pyrite and chalcopyrite composite, myrmekitic and trellis intergrowths (Table 6). Pyrrhotite occurs as Wormy-like and blebs growing in amphibole (Figure 3d). Discrete crystals or fine blebs and needles of pyrrhotite exsolution arranged in two sets along the cleavage planes of amphiboles are sometimes observed (Figure 2e). Pentlandite forms minute exsolution flames in pyrrhotite or in chalcopyrite.

In Wadi Rahaba gabbros, the sulfides constitute about 4.5 - 6 vol. %, pyrite, chalcopyrite and minor pyrrhotite. Chalcopyrite and pyrite are the most common sulfide phase; usually occur as minute inclusions in the silicates or as composite grains (Fig. 3f), mostly cracked and altered to goethite. Pyrrhotite is pinkish tan (in reflected light), sometimes partly or completely replaced by goethite along grain boundaries.

The sulfides in Imliq gabbros (3.4 - 4 vol. %) are represented by pyrite and chalcopyrite. Pyrite and chalcopyrite usually occur either as fine scattered disseminations or as specks adjacent each others in the mafic minerals. The sulphides minerals in El-Khamila gabbros include pyrite and chalcopyrite (2.5 - 4 vol. %). Chalcopyrite forms small inclusions in the silicates or anhedral grains commonly intergrowths with titanomagnetite to give chalcopyrite-titanomagnetite sandwich intergrowth (Figure 2g). Both pyrite and chalcopyrite are intergrown with ilmenite to give composite grains (Figure 2h). Blades of brassy yellow chalcopyrite are sometimes recorded.

RESULTS

I- Fe-Ti oxides

The derivation and evolution of the magma from which the gabbroic rocks was formed has been thoroughly documented (El-Metwally, 1992, 1997; Abdel-Karim, in preparation and others). However, the general Fe-Ti oxides compositions and their relations with magma evolution are still unsettled. The stages of relative magmatic evolution of all the studied samples can be roughly worked out using the correlation of relative contents of elements in the Fe-Ti oxides and sulfide minerals.

Based on the chemical characteristics, it can distinguish the analyzed Fe-Ti oxides from the gabbros in five areas in south Sinai into magnetite, ilmenite and titanomagnetite (Figure 4). The magnetite is characterized by high FeO and very low TiO₂ contents with respect to that of ilmenite and titanomagnetite (Figure 4). Moreover, the titanomagnetite is characterized by high TiO₂ and low FeO contents as compared with ilmenite of the studied areas (Figure 4).

Magnetite

Al₂O₃ and FeO contents in magnetite show a sharp increase coincident with the change in TiO₂. However, reverse relations are proved for FeO, MnO, V₂O₃ and The derivation and evolution of the magma from which the gabbroic rocks was formed has been thoroughly documented (El-Metwally, 1992, 1997; Abdel-Karim, in preparation and others). However, the general Fe-Ti Cr₂O₃ (Figure 5) versus TiO₂, probably as a function of temperature and composition.

Ilmenite-titanomagnetite

SiO₂ and FeO^t, Cr₂O₃ and MnO contents in ilmenite and titanomagnetite decrease, while V₂O₃ increases with increasing TiO₂, probably as a function of temperature and composition (Figure 6).

Ilmenite-Magnetite- titanomagnetite

Figure 7 shows the compositional variation of Fe-Ti oxide

Table 5. Results of microprobe analysis of the chalcopyrite of some gabbros from south Sinai, Egypt.

Element %	W. Nakhil			El-Khamila		W. Rahaba			Imliq		W. Tweiba			
	1	2	3	4	5	6	7	8	9	10	11	12	13	14
As	0.11	0.13	0.14	0.09	0.10	0.11	0.12	0.12	0.12	0.11	0.12	0.11	0.11	0.11
Fe	29.88	30.56	30.07	30.21	31.10	29.89	30.89	30.42	30.35	30.22	30.69	30.17	30.78	30.18
Cu	33.76	33.92	34.48	34.14	34.15	35.02	34.19	33.94	34.13	34.36	34.27	34.37	34.16	34.44
Cd	0.00	0.00	0.27	0.37	0.00	0.00	0.00	0.00	0.09	0.12	0.09	0.12	0.03	0.04
Co	0.08	0.07	0.07	0.03	0.02	0.04	0.02	0.04	0.06	0.05	0.04	0.04	0.03	0.04
Ni	0.18	0.17	0.16	0.07	0.08	0.08	0.07	0.06	0.14	0.11	0.10	0.07	0.10	0.08
S	34.27	34.94	34.28	35.02	34.45	34.81	34.65	34.92	34.33	34.92	34.46	34.92	34.48	34.88
Total	98.28	99.79	99.47	99.93	99.90	99.95	99.94	99.50	99.21	99.89	99.77	99.79	99.68	99.78

Table 6. Results of microprobe analysis of the pyrrhotite and pentlandite of some gabbros from south Sinai, Egypt.

Element %	Pyrrhotite								Pentlandite							
	W. Nakhil			W. Rahaba			W. Tweiba		W. Nakhil			W. Tweiba				
	1	2	3	4	5	6	7	8	1	2	3	4	5	6	7	8
As	0.71	0.69	0.42	0.71	0.57	0.70	0.49	0.71	0.72	0.67	0.73	0.71	0.72	0.70	0.72	0.71
Fe	61.33	58.85	58.44	58.94	59.89	58.90	59.16	58.92	29.39	29.57	28.97	30.08	29.48	29.71	29.39	29.73
Cu	0.10	0.09	0.11	0.10	0.11	0.10	0.11	0.10	0.08	0.09	0.12	0.11	0.10	0.10	0.11	0.11
Co	0.11	0.15	0.12	0.13	0.12	0.14	0.12	0.14	0.08	0.11	0.09	0.14	0.10	0.12	0.10	0.12
Ni	0.58	0.67	0.63	0.56	0.61	0.62	0.62	0.59	36.30	36.24	36.55	35.68	36.18	36.03	36.25	35.99
S	36.67	39.15	40.21	39.24	38.44	39.20	39.33	39.22	33.24	33.26	33.38	33.24	33.29	33.26	33.31	33.27
Total	99.50	99.60	99.93	99.68	99.72	99.64	99.82	99.66	99.81	99.94	99.84	99.96	99.87	99.92	99.88	99.92

phases in $MnO-V_2O_3-Cr_2O_3$ and $SiO_2-V_2O_3-Cr_2O_3$ diagrams. The analyzed Fe-Ti oxide phases display a relatively gradual increase in MnO with an equal amount of V_2O_3 and Cr_2O_3 from ilmenite and titanomagnetite to magnetite (Figure 7a). Meanwhile a simultaneous growth as well as a progressive evolution in the chemical compositions of ilmenite and magnetite (and less common titanomagnetite) in the studied areas is recorded with increasing SiO_2 (Figure 7b). This feature can be correlated with the magmatic evolution of the present gabbros.

The overall chemical results are illustrated by tie lines in Figure 8 to show equilibrium of the oxides in the triangle $TiO_2-FeO-Fe_2O_3$ under variable temperature conditions. These values were obtained qualitatively from typical analyses of oxide grains, as much as possible including minor exsolution lamellae, and will be followed up by more precise estimates based on modal analysis of oxide grains. On this diagram, the analyzed ilmenite plots on the ferranilmenite line formed by continuous solid solution above 800°C, meanwhile, the analyzed magnetite and Ti-magnetite plot close to the magnetite lie at the end of continuous solid solution above 600°C.

Magmatic intergrowths of Ti-magnetite and magnetite are observed (Figure 2a). After oxidation, both phases were exsolved to form high Ti and low Ti constituents. The simultaneous growth of Ti-magnetite and magnetite may point to oxidizing conditions in the magmatic chamber as concluded by Frost and Lindsley (1992).

Figure 8 also depicts the composition of Fe-Ti oxides in the $TiO_2-FeO-Fe_2O_3$ system diagram. The analyzed ilmenite, magnetite and titanomagnetite are plotted in the diagram with the tie lines connecting the analyses points of the coexisting phases. It is clear from this figure that the ilmenite in the all studied areas plots near the position of ilmenite exhibiting equal amounts of TiO_2 and FeO, while the magnetite and titanomagnetite lies close to the $FeO-Fe_2O_3$ sideline similar to magnetite.

II- Sulfides

The derivation and evolution of the magma from which the gabbroic rocks was formed has been thoroughly documented (El-Metwally, 1992, 1997; Mehanna et al., 2004; Abdel-Karim, in preparation and others). However, the general sulfide compositions and their relations with magma evolution are still unsettled. Nevertheless, the stages of relative magmatic evolution of all studied samples can be roughly worked out using the correlation of relative contents of elements in the sulfide minerals.

Pyrite-chalcopyrite

Based on the chemical characteristics, it can distinguish each of the analyzed pyrite and chalcopyrite into two types (Figures 9 and 10).

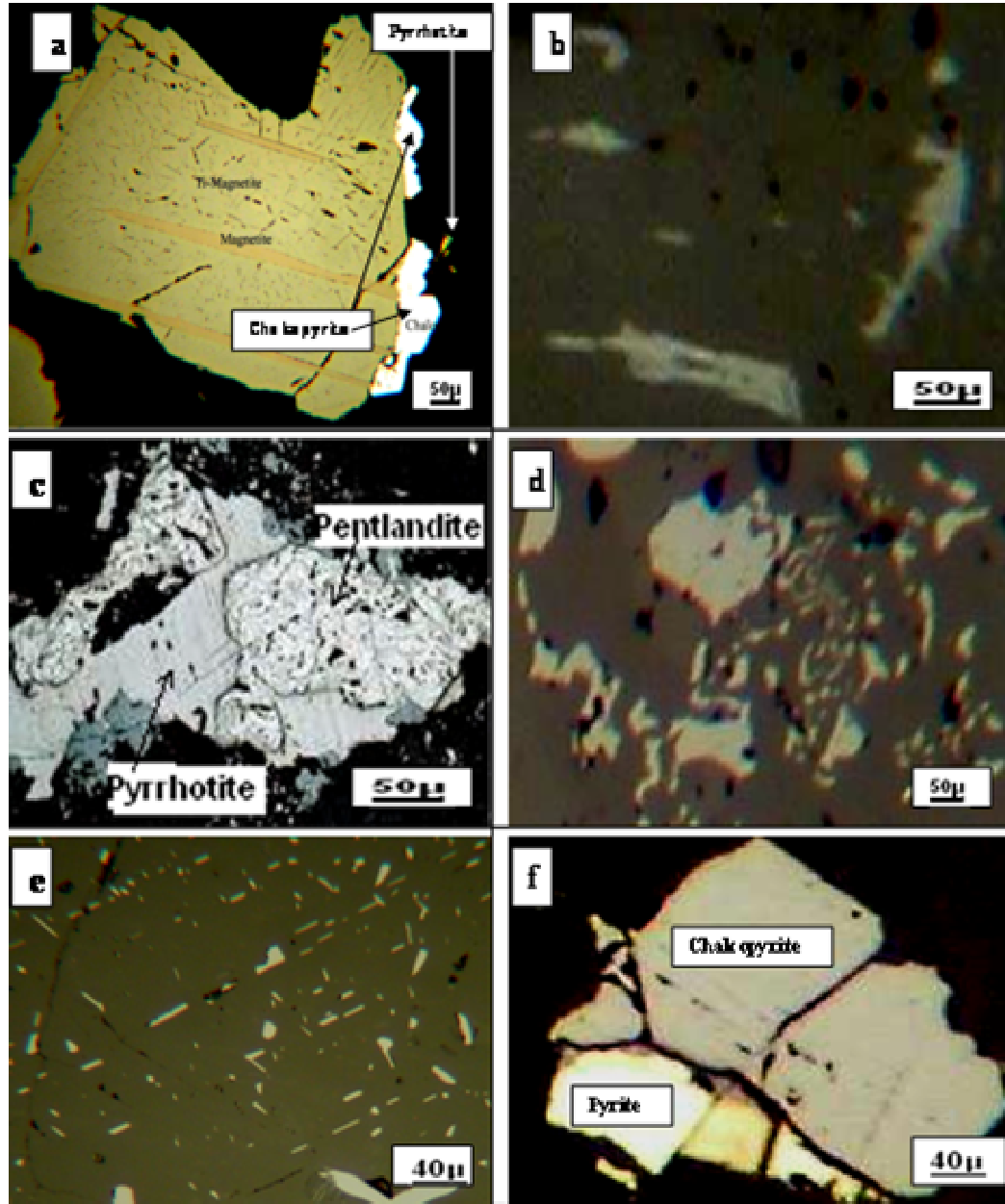


Figure 3. Photomicrographs showing the textures of sulfide minerals. **a)** irregular grains of chalcopyrite and pyrrhotite growing along the periphery of titanomagnetite-magnetite intergrowth, W. Tweiba, **b)** White flame patches of pyrrhotite, **c)** Pyrrhotite encloses pentlandite, W. Tweiba, **d)** Wormy-like and blebs of pyrrhotite exsolution growing in amphibole, W. Nakhil, **e)** Fine blebs and needles of pyrrhotite exsolution arranged along cleavage planes of amphibole, W. Nakhil, **f)** Pyrite-chalcopyrite composite grain, W. Rahaba.

Type I pyrite (Ni-rich) which recorded in Imliq and W. Nakhil localities which displays compositional variation ranging from 0.23 - 0.38% Ni, 0.04 - 0.10% As, 0.12 - 0.16% Co and 52.05 - 54.05% S.

Type II (Ni-poor) is recorded in Tweiba, W. Rahaba and El-Khamila localities and varies in composition from 0.02 - 0.07% Ni, 0.12 - 0.18% As, 0.22 - 0.27% Co and 52.34 - 54.25% S.

All these features probably suggest that both types cannot be co-magmatic origin (Figures 9 and 10). Ni/Cu ratio in type I pyrite is mostly >1, compared with that of type II (<1).

Type I chalcopyrite (Ni-rich) which recorded also in Imliq and W. Nakhil localities ranges from 0.13 - 0.18% Ni, 0.11 - 0.14% As, 0.05 - 0.08% Co and 34.27 - 34.94% S.

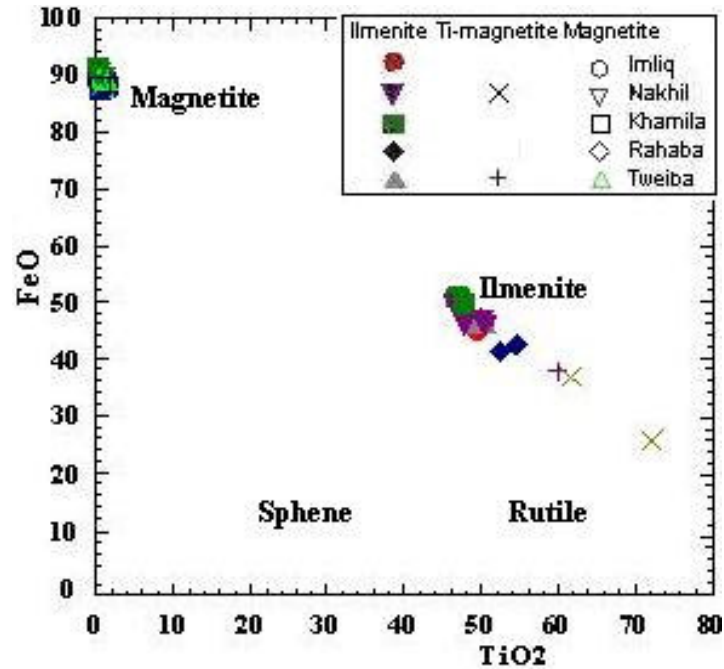


Figure 4. FeO-TiO₂ diagram for the studied Fe-Ti oxides of younger gabbros in five areas in south Sinai.

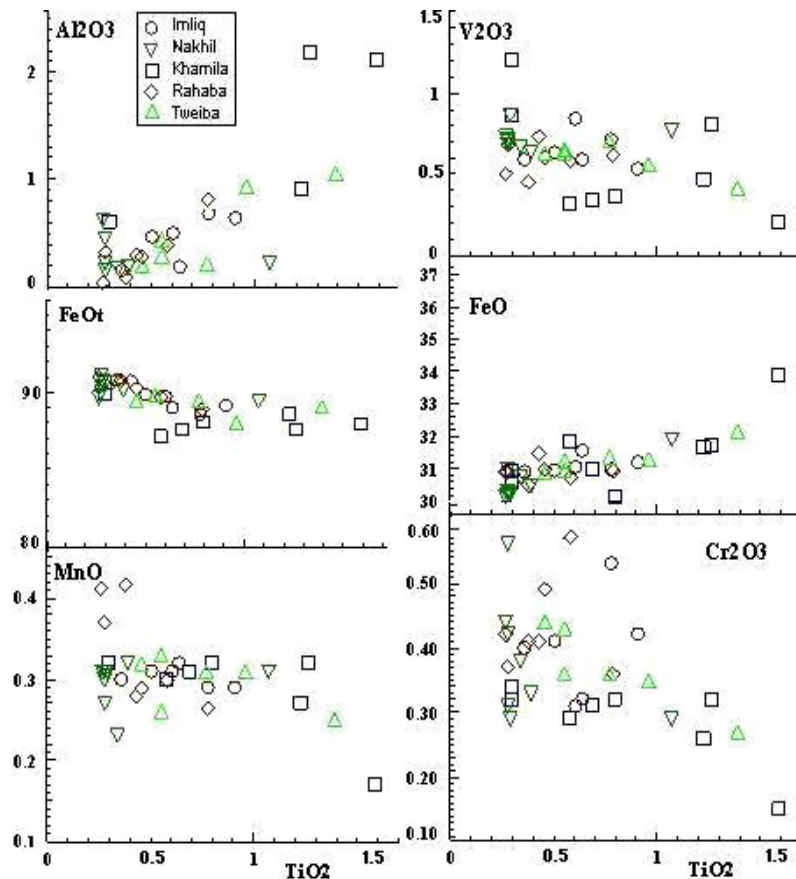


Figure 5. Chemical analyses of some oxides (wt. %) of magnetite plotted against TiO₂ (wt. %) from younger gabbros in five areas in south Sinai.

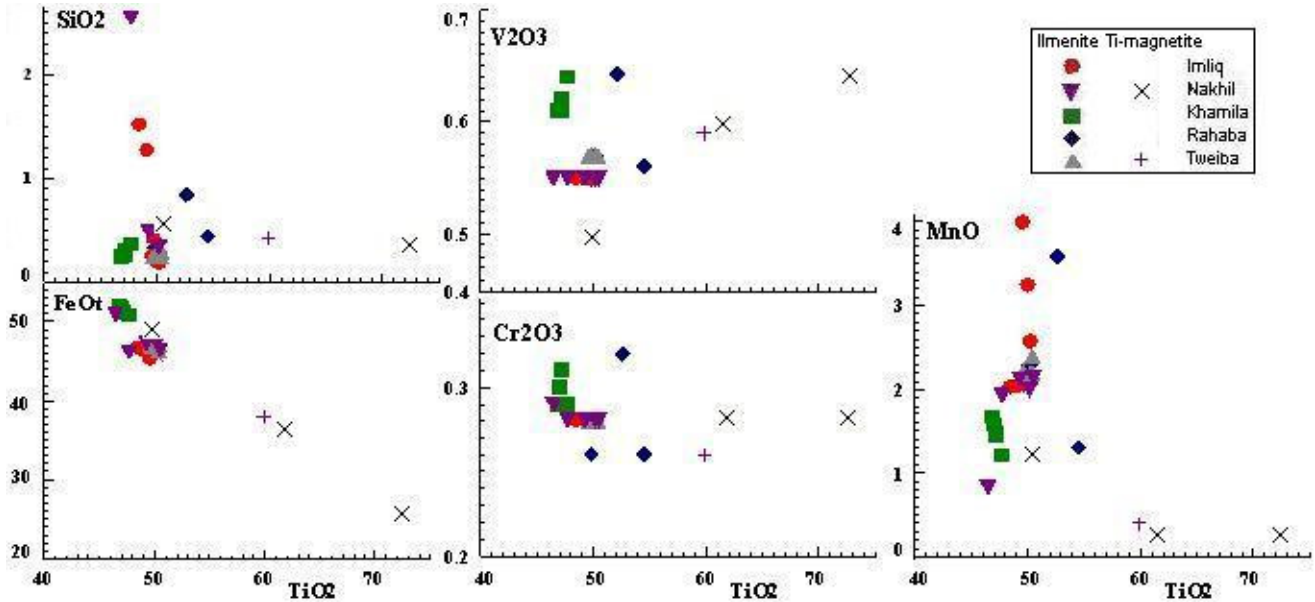


Figure 6. Chemical analyses of some oxides (wt. %) of ilmenite and titanomagnetite plotted against TiO_2 (wt. %) from younger gabbros in five areas in south Sinai

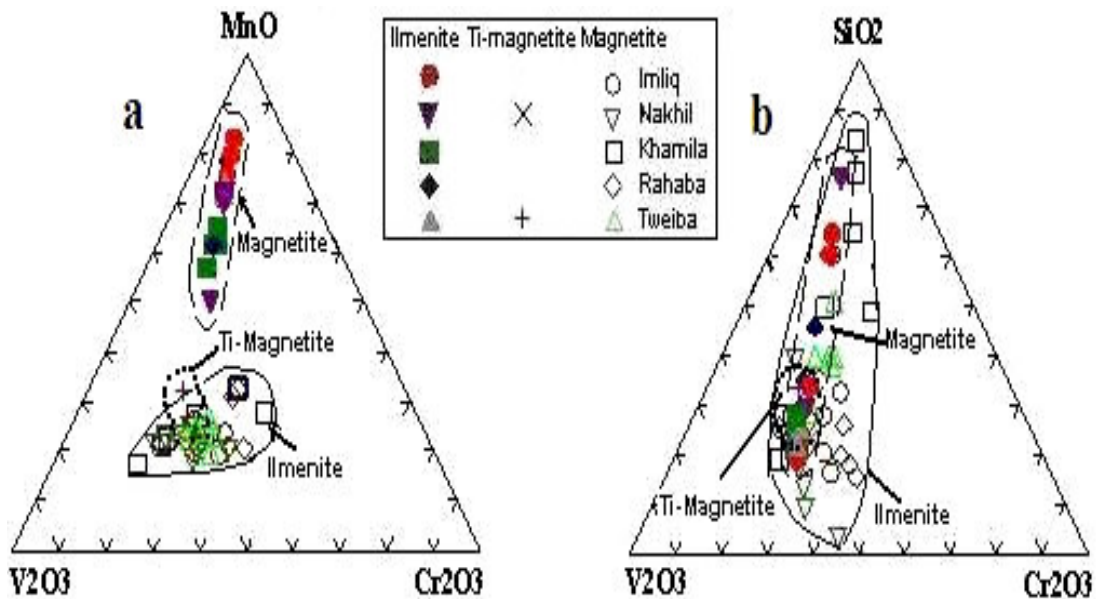


Figure 7. $\text{MnO-V}_2\text{O}_3\text{-Cr}_2\text{O}_3$ and $\text{SiO}_2\text{-V}_2\text{O}_3\text{-Cr}_2\text{O}_3$ system diagrams showing the compositional variation of analyzed Fe-Ti oxides of the younger gabbros in five areas in south Sinai.

Type II chalcopyrite (Ni-poor) which recorded in El-Khamila, W. Rahaba and W. Tweiiba localities varies from 0.02 - 0.10 Ni, 0.02 - 0.04 Co and 0.09 - 0.12% As (Table 5).

Ni in pyrite shows a sharp decrease coincident with the change in As and Co composition. However, reverse relations are proved for the chalcopyrite (Figure 9). Fe and Cu compositions in chalcopyrite are relatively constant

against Ni, as a function of temperature and composition changes. Moreover, same features are indicated between S composition in chalcopyrite and each of Ni, Co and As (Figure 10). Cu and Ni are both chalcophile and siderophile, partitioning strongly into sulfide phases in a magmatic system (Miller and Cervantes, 2002).

The chalcopyrite is also characterized by high Cu and low Co, Fe and S contents with respect to that of pyrite

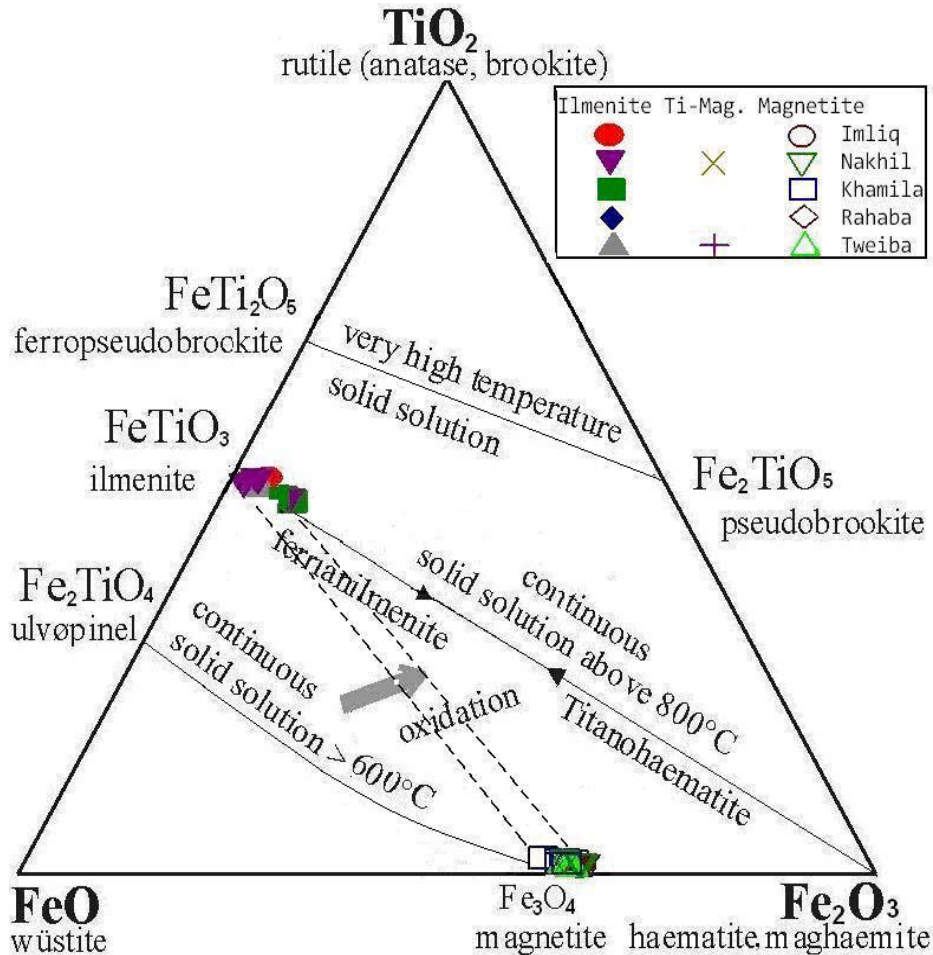


Figure 8. $\text{TiO}_2\text{-FeO-Fe}_2\text{O}_3$ solid system diagram showing the composition and approximate equilibrium tie lines (dashed lines) between analyzed ilmenite and magnetite from younger gabbros in five areas in south Sinai (modified after Buddington and Lindsley, 1964, Broska et al., 2003).

(Figures 9 and 10). It displays constant correlation between S and each of Ni, Co and As, probably due to the change in temperature and composition.

This result consistent with the detailed geochemistry carried out on the same five gabbros localities (Abdel-Karim, in prep.) which indicated their derivation from two independent magmas, example, tholeiitic (W. Tweiba, W. Rahaba and El-Khamila) and calc-alkaline (Imliq and W. Nakhil).

On the As-Ni-Co system diagram, the Ni-rich (type I) pyrite plots close to the Ni-Co sideline while the Ni-poor (type II) one lies close to the Co-As sideline. On the other hand, type I and II chalcopyrite, plot near the As-Ni sideline (Figure 11). Moreover, on the S-F-Cu system diagram the both kinds of pyrite plot in the midway of the S-Fe sideline showing relatively equal amounts of each of them. The chalcopyrite lies in the central portion of diagram exhibiting equal amounts of each of S, Fe and Cu (Figure 11).

Pyrrhotite-pentlandite

Pyrrhotite is a common mineral of magmatic sulfide segregations, occurs in basic igneous rocks as a late-stage fractional differentiate. Two types of pyrrhotite can be distinguished, type I (As-rich, 0.69 - 0.72) and type II (As-poor, 0.42 - 0.52). Type I is generally characterized by high Co contents (0.11 - 0.14) as compared with type II (0.12) (Table 6, Figure 12).

Pyrrhotite is generally characterized by high Fe (58.44 - 61.33%) and Co (0.11 - 0.15%) contents as compared with that of pentlandite (28.97 - 30.08% Fe) and (0.08 - 0.14% Co) respectively (Table 6). Co in pentlandite is usually substituting for Fe. Ni in pentlandite (35.68 - 36.55%) is strongly higher than that of pyrrhotite (0.58 - 0.67%). Therefore, pentlandite is considered as an important ore of nickel.

The plots of each of Ni and S against some other elements (Figure 12) show a steady increase As, Co and Cu

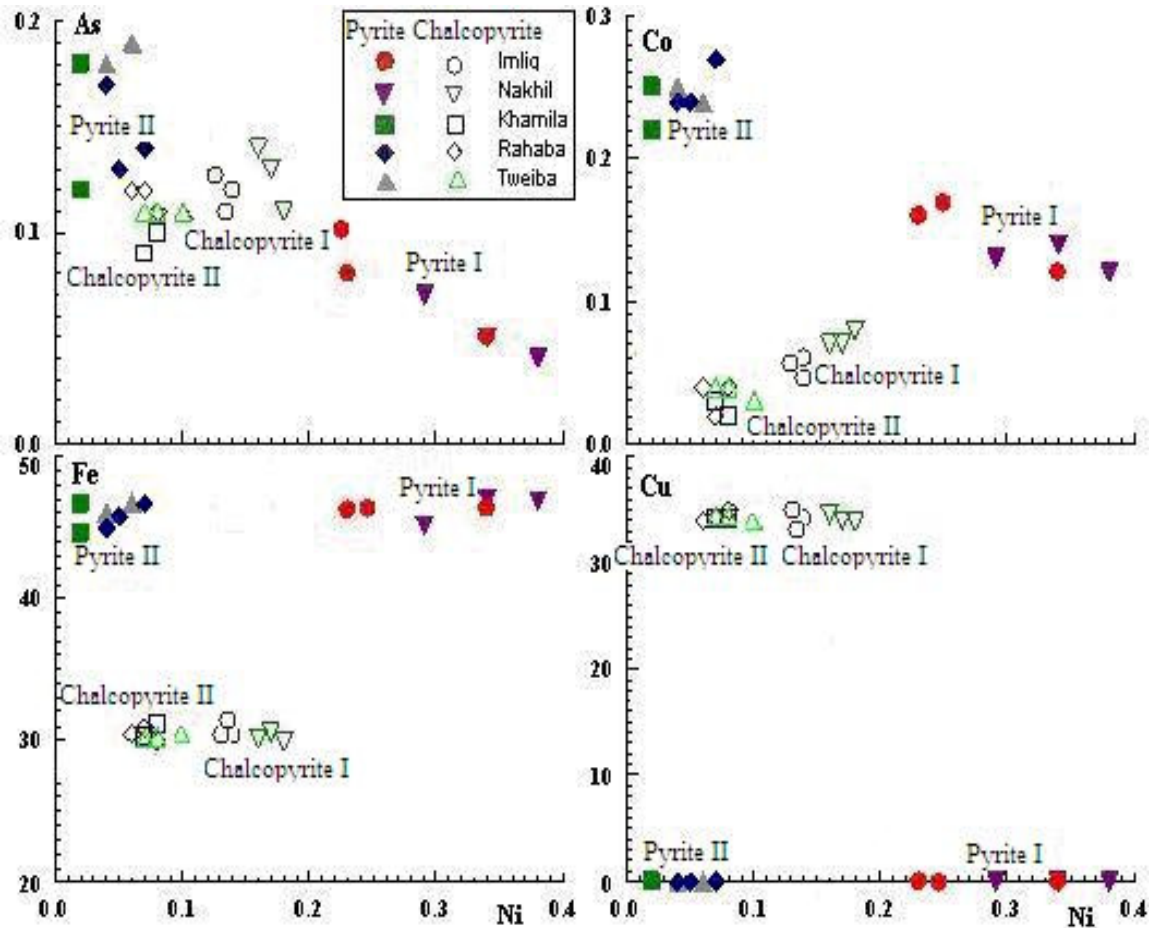


Figure 9. Chemical analyses of some elements (wt. %) of pyrite and chalcopyrite plotted against Ni (wt. %) from younger gabbros in five areas in south Sinai.

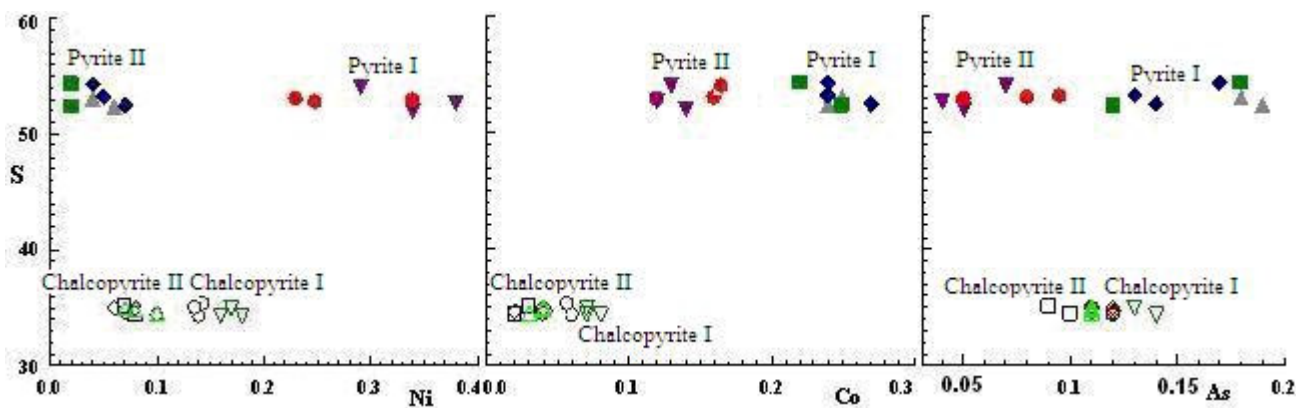


Figure 10. Chemical of some elements (wt. %) of pyrite and chalcopyrite plotted against S (wt. %) from younger gabbros in five areas in south Sinai

compositions in each of pyrrhotite and pentlandite with constant Ni. S composition in pyrrhotite slightly decreases with increasing As and Fe, but it increases with increasing Co. On the other hand, S composition is relatively constant with increasing As and Co.

Figure (13a) depicts the composition of sulfide phases in S-Fe-Ni diagram. The analyzed pyrite, chalcopyrite, pyrrhotite and pentlandite are plotted in the diagram with the tie lines connecting the analyses points of the co-existing phases. It is clear from this figure that the pyrite,

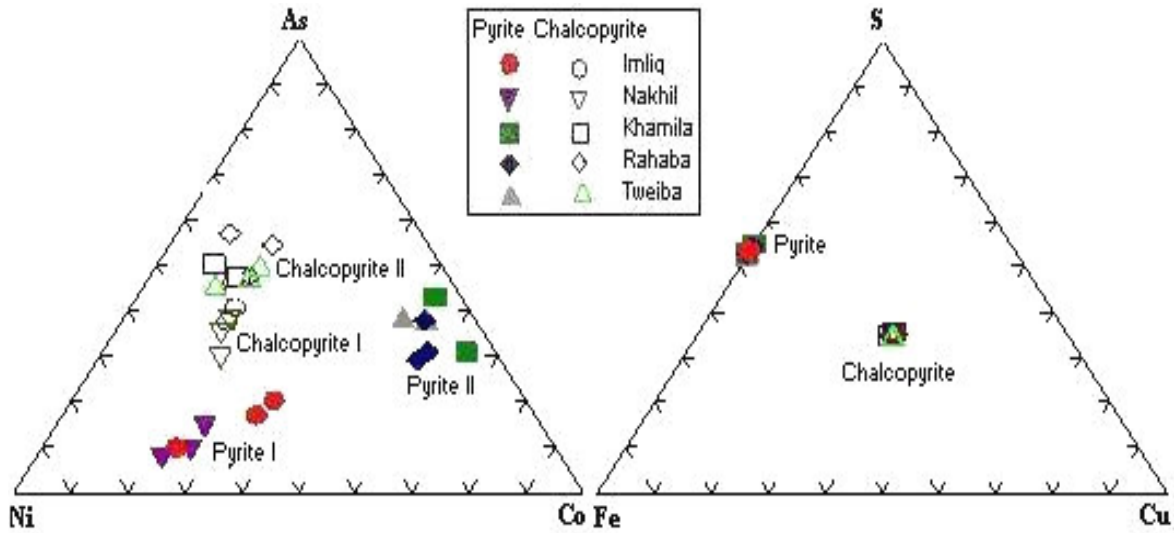


Figure 11. As-Ni-Co and S-Fe-Co system diagrams showing the composition of analyzed pyrite and chalcopyrite from younger gabbros in five areas in south Sinai.

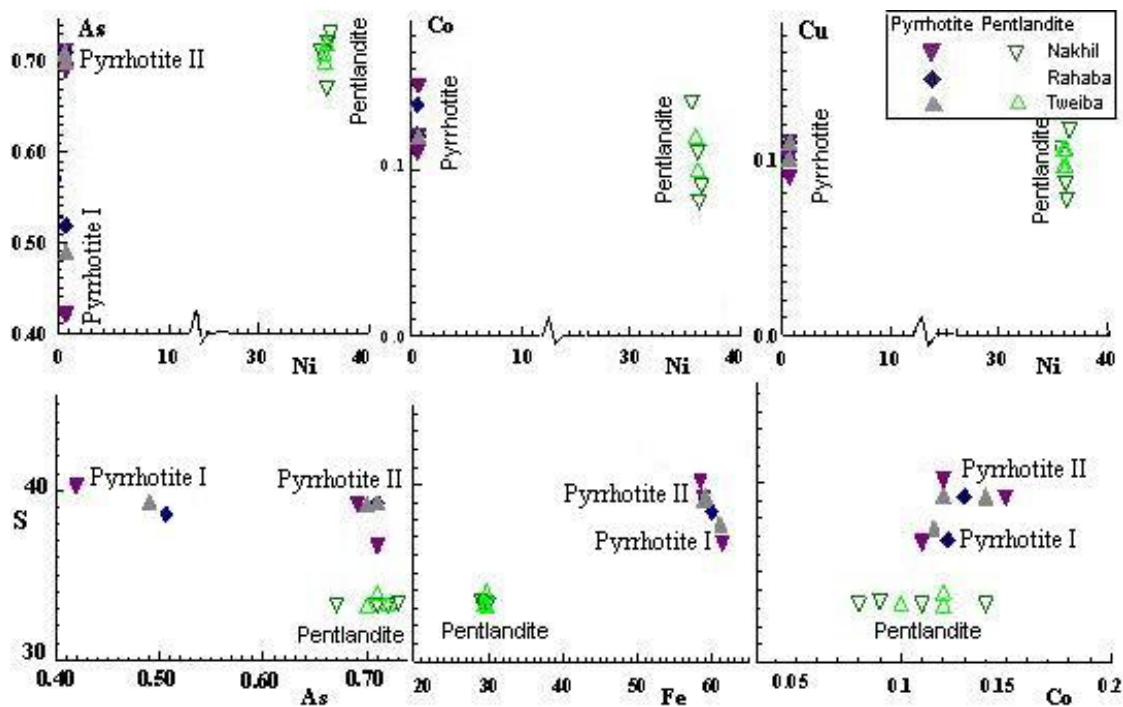


Figure 12. Chemical analyses of some elements (wt.%) of pyrrhotite and pentlandite plotted against Ni and S (wt. %) from younger gabbros in five areas in south Sinai.

chalcopyrite and pyrrhotite have chemical compositions lay relatively in the middle portion of S-Fe line, while the composition of pentlandite fall in the central portion of the S-Fe-Ni system.

Figure (13b) shows the decrease of Ni contents with the evolution of As and Cu which correlate with the evolution of the present mafic magma. As contents increase with decrease of Ni from pentlandite thought pyrite I, pyrrhotite I and II

to pyrite II as the magmatic evolution change from tholeiitic (W. Tweiba, W. Rahaba and El-Khamila) to calc-alkaline (Imliq and W. Nakhil) suites.

DISCUSSION

Disseminated Fe-Ti oxides and sulfides were discussed in the present study. The composition of the Fe-Ti oxide

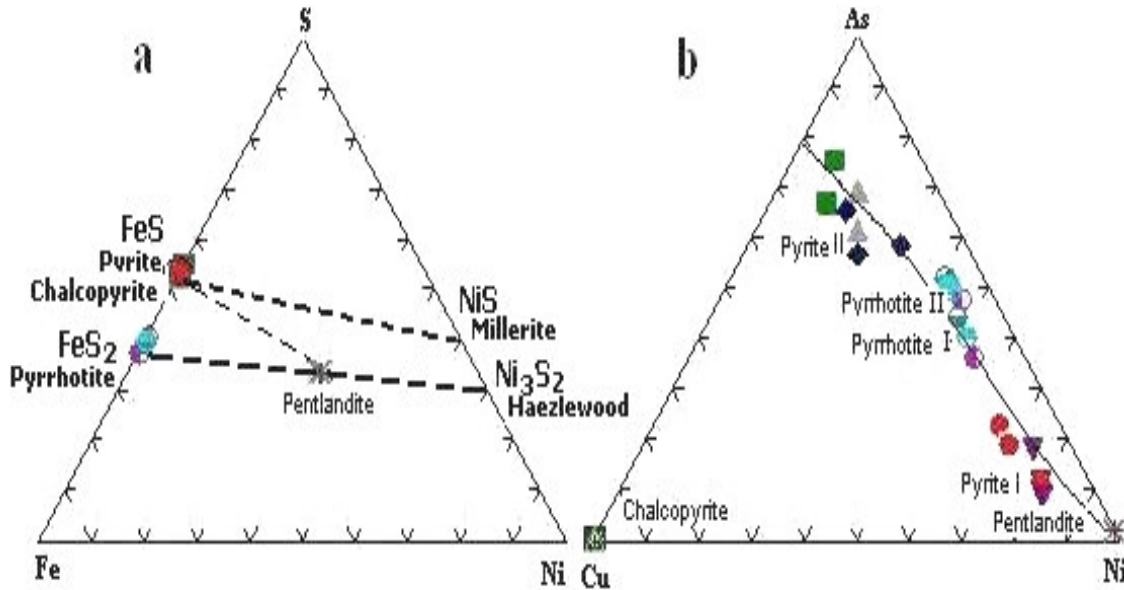


Figure 13-a). S-Fe-Ni (Modified after Halkoaho et al., 1990) and, **b)** As-Cu-Ni ternary solid solution systems showing the composition of sulfides from the studied younger gabbros in five areas of south Sinai.

minerals was considerably modified during the cooling of the intrusions by means of intracrystalline exchange reactions (Hassan, 2003). During cooling of the intrusions, oxidation caused the exsolution of magnetite from titanomagnetite solid solution, forming either distinct lamellae of magnetite in titanomagnetite or granular exsolution of ilmenite around grains of magnetite. Disseminated sulfide minerals are associated with oxides in some of studied intrusions.

The formation of ilmenite trellis and lamellae in magnetite and titanomagnetite is due to an oxidation process (Anderson, 1968; Al-Mohandis, 1980) which may attribute to: i- excess of oxygen contained in titanomagnetite; ii- trapped oxidizing agents and iii- introduction of an external oxidizing agent. This feature may indicate that the parental magma crystallized under conditions of high P_{H_2O} and oxygen fugacity, as suggested by modal increase of hydrous minerals (McSween and Nystrom, 1979) such as primary hornblende and biotite in hornblende- and pyroxene hornblende gabbros of Wadi Tweiba and Nakhil areas. Also the presence of hypersthene and pigeonite in uraltized- and olivine gabbros of Wadi Rahaba and El-Khamila areas indicate increasing oxygen fugacity of the magma (Wilson, 1989).

These compositions were in equilibrium with a fractionated tholeiitic and calc-alkaline magmas saturated in Fe-Ti oxides and sulfides. Simulations of the whole rock geochemistry obtained by Abdel-Karim (in prep.) shows that the oxide-rich rocks can be modeled by crystal fractionation and differentiation with prominent crustal contaminated tholeiitic magma and calc-alkaline parental magma followed by accumulation of disseminated oxides and sulfides and silicate phases in equilibrium with the fractionated magma. Oxidation causes the conversion of Fe^{2+} to

Fe^{3+} and results in the crystallization of magnetite. Accumulation of magnetite brings about a decrease in Fe in the fractionation liquid, which then favors the saturation of the magma in sulfides.

Progressive differentiation of liquids residual from calc-alkaline (noritic) magmas leads to late enrichment in Fe-Ti oxides and Co-Ni-Cu sulfides. Typically plagioclase crystallization results in concentration of Fe and Ti in residual magmas which typically crystallize to form tholeiitic (ferrodioritic and ferrogabbroic) magma. Disseminated deposits are believed to have formed in-situ. An emplacement as Fe-Ti-oxide- and sulfide-rich immiscible melt with little silica is the proposed genetic model.

Magmatic sulfide deposits (Ni-Cu-Co) are commonly hosted by mafic igneous rocks. The sulfides occur mostly as monomineralic grains less than 70 μm in size included in hydrosilicates or attached to the grain boundaries of Fe-Ti oxides. A few sulfide grains are included in or sandwiched by Fe-Ti oxides. The sulfides are the result of the separation of an immiscible sulfide melt from the sulfur-saturated silicate melt.

Chalcopyrite, pyrite, pyrrhotite and pentlandite are the main minerals in magmatic sulfide deposits of the present gabbroic rocks.

Sulfide mineralization was subdivided into groups based on the three most common assemblages (Miller and Cervantes, 2002):

1. Armored (completely encased in a silicate phase in the two dimensions visible on the surface of the thin section), irregular to rounded or oblong, generally multiphase globules ranging from a few tens to a few hundred micrometers across, without reaction coronas.
2. Similarly shaped and sized globules hosted in brown

amphibole, commonly, but not exclusively, at the contact between fresh igneous phases.

3. Sub-rectangular to angular, predominantly single-phase small grains, as inclusions along cleavage and fractures, and interstitial to and intermixed with fresh igneous phases.

The third group although generally the least abundant, was present in every section examined and probably represents secondary mineralization. The sulfides armored in plagioclase or pyroxene are the next most common morphology in terms of the number of thin sections where they were recognized, but sulfides armored in olivine are exceedingly rare. However, few sulfides are present in association with translucent brown amphibole.

According to Mazdab and Force (1998), comparison of Co/Ni ratios in sulfides readily differentiate Fe oxide deposits (Co/Ni >1) from magmatic Fe-Ti oxide or magmatic immiscible sulfide Ni-Fe-Cu systems (Co/Ni <1). Most of the analyzed samples in this study have a Co/Ni < 1, indicating that they are magmatic.

Formation of the present deposits begins with the melting of hot mantle rising. The melting produces basaltic magma that is relatively rich in metals but may be poor in sulfur, which then rises upward and intrudes into the crust, forming two magma chambers (tholeiitic and calc-alkaline suites). Both magmas may variably interact with the crust and become contaminated. Sulfur from surrounding rocks may be incorporated into the magmas. This contamination reduces the ability of the magmas to keep sulfur in solution, and the magma may variably become sulfur saturated. When sulfur saturation occurs, droplets and blebs of sulfide liquid form. As the sulfide droplets segregate, they scavenge metals such as Co, Ni and Cu from the magma. If these sulfide droplets become sufficiently concentrated, a magmatic sulfide deposit is formed. This result is consistent with the recent studies at Noril'sk, Voisey Bay and other deposits (Naldrett et al., 1998 and Lambert et al., 2000).

The analyzed ilmenite plots on the ferranilmenite line formed by continuous solid solution above 800°C, meanwhile, the analyzed magnetite and Ti-magnetite plot close to the magnetite lie on the end of continuous solid solution above 600°C (Figure 8). These results are typical of mafic igneous intrusions (Hassan, 2003).

The base metals sulfides are often associated with any magma, first in the form of monosulfide solid solution (Fe, Ni, Cu) S, at temperatures start from magmatic to late magmatic (down to 600°C). During cooling, the monosulfide solid solution decomposes to pyrrhotite, pentlandite and chalcopyrite at temperatures down to 300°C. This scenario is acceptable and experimentally proved by many workers (Kissin and Scott, 1982, Sinyakova et al., 1997, Kojonen et al., 2003 and others).

According to Craig and Kullerud (1969), the sulfide assemblage of pyrite, chalcopyrite, pyrrhotite and pentlandite is typical of igneous sulfides segregated from mafic magmas. The absence of troilite may indicate that the

present sulfides have not undergone lower temperature re-equilibration. This also indicates that the pyrrhotite was originally quite Fe rich (58.40-61.33 wt%, present study) and have not exhibited troilite exsolution at low temperature (Kissin and Scott, 1982). Therefore, the expected condition of formation of the present sulfides is most probably of ~ 600°C with a final equilibration above 140°C.

Conclusion

The present petrographic and chemical investigations carried out on the Fe-Ti oxides and sulfides in the vicinity of south Sinai, offered new data about the type of mineralization related to the younger gabbros. Microscopic and electron microprobe studies made it possible to obtain the composition of the minerals, their textures and genesis as well as condition of formation. This investigation can be summarized as follows:

Exsolution of magnetite from the titanomagnetite solid solution, forming either distinct lamellae of magnetite in titanomagnetite or granular exsolution of ilmenite around grains of magnetite were developed by oxidation during cooling of the intrusions. Also, the formation of ilmenite trellis and lamellae in magnetite and titanomagnetite indicate again an oxidation process which attribute to excess of oxygen contained in titanomagnetite; trapped oxidizing agents and introduction of an external oxidizing agent. This feature may indicate the high PH_2O and oxygen fugacity of the parental magma, as suggested by modal increase of hydrous hornblende and biotite and the presence of hypersthene and pigeonite.

The sulfides occur mostly as monomineralic grains less than 70 µm in size included in hydrosilicates or attached to the grain boundaries of Fe-Ti oxides. A few sulfide grains are included in or sandwiched by Fe-Ti oxides. The cumulus minerals are clinopyroxene and orthopyroxene ± olivine, the intercumulus minerals are orthopyroxene, plagioclase, hornblende and minor biotite. The Fe-Ti oxides and sulfides are located in the intercumulus spaces of the host rocks.

The Co/Ni values of the studied sulfides suggest that they were formed in a magmatic immiscible sulfide Ni-Fe-Cu system. The present igneous sulfides reported from the five localities include pyrite, chalcopyrite, pyrrhotite and pentlandite. These sulfides can be interpreted to have formed predominantly by accumulation of immiscible magmatic sulfide droplets.

Based on the chemical characteristics, it can distinguish each of the analyzed pyrite and chalcopyrite into two types (Ni-rich pyrite and chalcopyrite, and Ni-poor pyrite and chalcopyrite).

Ni-rich pyrite and chalcopyrite are associated with the tholeiitic gabbros dominated in El-Khamila, Wadis Tweiba and Nakhil, while the Ni-poor pyrite and chalcopyrite are characteristic of the calc-alkaline gabbros from Imliq and Wadi Nakhil areas.

The Fe-Ti oxides are believed to have been formed under temperature of ~ 800°C for ilmenite and ~ 600°C for magnetite.

The analyzed pyrrhotite is stoichiometrically close to Fe₇S₈ and contains 0.56 to 0.62 wt% Ni. Moreover, there are no evidences for the existence of troilite neither from microscopic nor from chemical investigation. The expected temperature of formation of the present sulfide assemblage is most probably below 600°C, with a final equilibration above 140°C.

REFERENCES

- Al-Mohandis AA (1980). The opaque minerals of Jabal Sha layered intrusion. Saudi Arabia. J. Coll. Sci. Riyadh. 11: 171-188.
- Anderson AT (1968). The oxygen fugacity of alkaline basalt and related magmas Tristanda Cunha. Am. J. Sci. 266: 704-727.
- Basta EZ, Takla MA (1974). Distribution of opaque minerals and origin of the gabbroic rocks of Egypt. Bull. Fac. Sci., Cairo Univ. 47: 347-364.
- Broska I, Uher P, Ondrejka M (2003). Geochemical and mineralogical characterization of the Fe-Ti oxide paragenesis in the magmatic and hydrothermal systems. Slovak Academy of Sciences. Web page: geol.sav.sk/.
- Buddington AF, Linsley DH (1964). Iron-titanium oxides minerals and synthetic equivalents. J. Petrol. 5: 310-357.
- Bugrov VA, Shalaby IM (1973). First discovery of Cu-Ni mineralization in gabbro-peridotite rocks in Eastern Desert of Egypt. Annals Geol. Surv. Egypt. 3: 177-183.
- Craig JR, Kullerud G (1969). Phase relations in the Cu-Fe-Ni-S system and their application to magmatic ore deposits. In Wilson HDB (Ed.): Magmatic Ore Deposits: A Symposium. Econ. Geol. Monogr. 4: 344-358.
- El-Gaby S (2005). Integrated evolution and rock classification of the Pan-African belt in Egypt. 1st Symposium on the classification of the basement complex of Egypt, Assuit Univ., Egypt, Proceedings pp. 1-9.
- El-Gaby S, List FK, Tehrani R (1988). Geology, evolution and metallogenesis of the Pan-African belt in Egypt. In El-Gaby S, Greiling RO (eds.): The Pan-African belt of the northeast Africa and adjacent areas, Vieweg, Verlag pp. 17-68.
- El-Mahallawi MM, Kamel OA, Helmy HM (1997). Petrology, geochemistry and petrogenesis of the host rocks of abu Swayel Cu-Ni-PGE mineralization, Eastern Desert, Egypt. Egypt. J. Geol. 41/1: 75-102.
- El-Mettawly A (1992). Pan-African post-orogenic gabbro cumulates from Sinai massif, "Egypt": geochemistry and mineral chemistry. J. African Earth Sci. 14/2: 217-225.
- El-Metwally AA (1997). Petrogenesis of gabbroic rock intrusions from south-central Sinai massif: A transition from arc to intraplate magmatism. The 3rd Intern. Conf. On Geochemistry, Alex. pp. 49-66.
- El-Ramly MF (1972). A new geological map for the basement rocks in the Eastern Desert and Southeastern Desert, Egypt. Geol. Surv. Egypt 2: 2-18.
- Frost BR, Lindsley DH (1992). Equilibria among Fe-Ti oxides, pyroxenes, olivine, and quartz: Part II. Application. American Mineralogist 77: 1004-1020.
- Halkoaho TAA, Alapieti TT, Lahtinen JJ (1990). The Sompjarvi PGE Reef in the Penikat layered intrusion, Northern Finland. Mineralogy and Petrology 42: 39-56.
- Hassan N (2003). Genèse des dépôts de Fe-Ti-P associés aux intrusions litées (exemples: l'intrusion mafique de Sept-Iles, au Québec; complexe de Duluth aux États-Unis). PH.D., Université du Québec à Chicoutimi à Montréal, 2003, <http://dx.doi.org/doi>.
- Heikal MTS, Shazly AG, Hussein HA, El-Aassy IE, El-Galy MM (1998). Characterization and petrogenesis of younger gabbros of Nuweiba-Dahab area, West Gulf of Aqaba, Sinai, Egypt. Egypt. J. Geol. 42/1: 15-37.
- Khalil SO (2005). The Egyptian gabbroic rocks. 1st Symposium on the classification of the basement complex of Egypt, Assuit Univ., Egypt Proc. pp. 49-51.
- Kissin SA, Scott SD (1982). Phase relations involving pyrrhotite below 350°C. Econ. Geol. 77: 1739-1754.
- Kojonen K, Gervilla F, Merkle RK (2003). Mineralogy of the Keivitsa Cu-Ni-PGE deposits, northern Finland. Abstract. EGS-EUG-AUG Joint Assembly, Nice April 2003, session VGP 330.
- Kroner A, Eyal M, Eyal Y (1990). Early Pan-African evolution of the basement around Elat (Israel) and the Sinai Peninsula revealed by single-zircon evaporation dating, and implication for crustal accretion rates. Geology 18: 545-548.
- Lambert DD, Frick LR, Foster JG, Li C, Naldrett AJ (2000). Re-Os Isotope Systematics of the Voisey's Bay Ni-Cu-Co Magmatic Sulfide System, Labrador, Canada: II. Implications for Parental Magma Chemistry, Ore Genesis, and Metal Redistribution. Econ. Geol. 95: 867-888.
- Mamoun KM, Soliman FA, Shendi EH, Khalil S, Nakagawa K (2004). Integrated geophysical exploration for sulphide minerals in the Wadi Sa'al area, south Sinai, Egypt. J. Geosci. Osaka City Univ. 47: 113-126.
- Mazdab FK, Force ER (1998). Comparison of cobalt and nickel contents in sulfides from iron-oxide (Cu-Au-U-REE) occurrences with others hydrothermal and magmatic systems. Abstr. Annu. Meet. Geol. Soc. Am. 30: 369. (Abstract).
- McSween HY, Nystrom PG (1979). Mineralogy and petrology of the Dutchmans Creek gabbroic intrusion, South California. Amer. Mineral 64: 531-545.
- Mehanna AM, Wateit MA, El-Amawy MA, Soliman F, Ghabour Y (2004). Petrogenesis and metamorphism of the basement rocks of Imlig area, Southwest Sinai, Egypt. Annals Geol. Surv. Egypt XXVII: 35-59.
- Miller DJ, Cervantes P (2002). Sulfide mineral chemistry and petrography and platinum group element composition in gabbroic rocks from the Southwest Indian Ridge. In Natland JH, Dick HJB, Miller DJ, Von Herzen RP (Eds.): Proc. ODP, Sci. Results, 176. Web. Page: <http://www-odp.tamu.edu/publications/176_SR/chap_07/chap_07.htm>.
- Naldrett A, Lightfoot P, Gorbachev NS (1998). A model for formation of the Ni-Cu-PGE deposits of the Noril'sk region. International Platinum. S-Petersburg, -Atheus. 92-106.
- Nasr BB, Sadek MF, Masoud MS (2000). Some new occurrences of layered titanomagnetite, Eastern Desert, Egypt. Annals Geol. Surv. Egypt XXIII: 679-690.
- Ramadan Kh, Niazy E (1997). Magnetite ore mineralization of Um Gheig area. Eastern Desert, Egypt. Egyptian Mineralogist 9: 133-145.
- Rasmy A (1982). Mineralogy of copper-nickel sulphide Mineralization at Akarem area, south Eastern Desert, Egypt. Ann. Geol. Surv. XII: 141-162.
- Sideek S, El Goresy A (1996). Phase relations of sulphides assemblages at Akarem area. Proc. Geol. Surv. Egypt Cenn. Conf. 759-773.
- Sinyakova EF, Kosyakov VI, Shestakov VA (1997). Liquidus surface of the Fe-Ni-S system at the XS < 51. Experiment in Geosciences 6/2: 57-58.
- Takla MA, Basta EZ, Fawzi, E (1981). Characterization of the older and younger gabbros of Egypt. Delta. J. Sci. 5: 279-314.
- Takla MA, Basta FF, Madbouly MI, Hussein AA (2001). Mafic-ultramafic intrusions of Sinai, Egypt. Annals Geol. Surv. Egypt. XXXIV: 1-40.
- Wilson M (1989). Igneous Petrogenesis. Hyndman, London p. 466.